

# Weight Functions Method application on a delta-wing X-31 configuration

Nicoleta ANTON<sup>1</sup> and Ruxandra Mihaela BOTEZ<sup>\*1</sup>

\*Corresponding author

<sup>\*1</sup> Ecole de Technologie Supérieure, Montréal, Canada, H3C 1K3  
Ruxandra.Botez@etsmtl.ca

DOI: 10.13111/2066-8201.2011.3.4.1

**Abstract:** *The stability analysis of an aircraft configuration is studied using a new system stability method called the weight function method. This new method finds a number of weight functions that are equal to the number of first-order differential equations. This method is applied for longitudinal and lateral motions on a delta-wing aircraft, the X-31, designed to break the "stall barrier". Aerodynamic coefficients and stability derivatives obtained using the Digital DATCOM code have been validated with the experimental Low-Speed Wind tunnel data obtained using the German–Dutch Wind Tunnel (DNW–NWB). Root Locus Method is used to validate the method proposed in this paper.*

**Key Words:** *aerodynamics, DATCOM, flight dynamics, root locus, stability derivatives, wind tunnel*

## 1. INTRODUCTION

Modern fighter aircraft are designed with an unstable configuration or a marginal stability, and control laws are needed to stabilise the aircraft. A new method for systems stability analysis, called the Weight Function Method, is used to analyse the longitudinal and lateral motions of the X-31.

The X-31 aircraft was designed to achieve its best performance, flexibility and effectiveness in air combat, due to its canard configuration that provided a better longitudinal manoeuvrability.

Its aerodynamics contains degrees of non linearity's that are representative for a modern fighter aircraft, that was designed to investigate its behaviour at high angles of attack (-5 to 56 degrees).

The mathematical model uses aerodynamic data obtained from wind tunnel tests and the results provided by Digital DATCOM code, for subsonic speeds.

Digital DATCOM code [1], known also as DATCOM+, is the first implementation of the DATCOM procedures in an automatic calculations code. The software is a directly executable portable application.

Input data, consisting of geometric and aerodynamic parameters of the aircraft, and flight conditions, are introduced through a text file called "*aircraft\_name.dcm*" whose format is specific to the software.

The DATCOM+ program calculates the static stability, the high lift and control, and the dynamic derivative characteristics.

This program applies to aircraft flying in the subsonic, transonic and supersonic regimes, more precisely to traditional wing–body–tail and canard– equipped aircraft.

The computer program offers a trim option that computes control deflections and aerodynamic data needed to trim the aircraft in the subsonic Mach regimes.

## 2. WEIGHT FUNCTION METHOD DESCRIPTION

In most practical problems, differential equations that model the behaviour of a dynamical system often depend on more than one parameter. The Lyapunov stability criterion is based on finding a Lyapunov function. It is not simple and is not always guaranteed to find a Lyapunov function. The Lyapunov method is very useful, however, when the linearization around the point of equilibrium leads to a matrix of evolution with eigenvalues having zero real parts [2].

The Weight Function Method (WFM) replaces the classical Lyapunov function finding problem with a method that finds a number of weight functions equal to the number of the first order differential equations modelling the system [2, 3]. The difference between the two methods is that the Lyapunov method finds all functions simultaneously, while the *weight functions method* finds one function at a time, with their total number equal to the number of the first order differential equations. For this reason WFM is found to be more efficient than the Lyapunov method.

For a better understanding of this method, its basic principle is defined in the next system of equations (1). The coefficients  $a_{1i}$ ,  $b_{1i}$ ,  $c_{1i}$ ,  $d_{1i}$ ,  $i = 1 \div 4$  contain the stability derivatives terms. The  $x_1, x_2, x_3, x_4$  represent the unknowns of the system of equations:

$$\begin{cases} f_1 = a_{11} x_1 + a_{12} x_2 + a_{13} x_3 + a_{14} x_4 \\ f_2 = b_{11} x_1 + b_{12} x_2 + b_{13} x_3 + b_{14} x_4 \\ f_3 = c_{11} x_1 + c_{12} x_2 + c_{13} x_3 + c_{14} x_4 \\ f_4 = d_{11} x_1 + d_{12} x_2 + d_{13} x_3 + d_{14} x_4 \end{cases} \quad (1)$$

The total weight function  $W = \sum_{k=1}^4 w_k x_k f_k$  is defined, in which  $w_1, w_2, w_3$  and  $w_4$  are

the weight functions whose sign should be negative to ensure the aircraft stability. In the aircraft model, the sign of the total function  $W$  given by eq. (2) should be negative to ensure the aircraft stability.

$$\begin{aligned} W = & w_1 x_1 (a_{11} x_1 + a_{12} x_2 + a_{13} x_3 + a_{14} x_4) + w_2 x_2 (b_{11} x_1 + b_{12} x_2 + b_{13} x_3 + b_{14} x_4) + \\ & + w_3 x_3 (c_{11} x_1 + c_{12} x_2 + c_{13} x_3 + c_{14} x_4) + w_4 x_4 (d_{11} x_1 + d_{12} x_2 + d_{13} x_3 + d_{14} x_4) \end{aligned} \quad (2)$$

In our paper, three of the four functions  $w_i$ :  $w_1, w_2$  and  $w_3$  will be positively defined based on the sign of the coefficients  $a_{1i}, b_{1i}, c_{1i}, d_{1i}$  with  $i = 1 \div 4$ . The last one will be constant and imposed by the author,  $w_4 > 0$ . If the positive weight functions will be well defined, then the sign of total function  $W$  will be analyzed in order to identify the stability or instability areas of the system.

## 3. APPLICATION ON X-31 AIRCRAFT

The X-31 aircraft was designed to break the "stall barrier", allowing the aircraft to remain under control at very high angles of attack. The X-31 aircraft employs thrust vectoring paddles which are placed in the jet exhaust, allowing its aerodynamic surfaces to maintain their control at very high angles.

For its control, the aircraft has a canard, a vertical tail with a conventional rudder, and wing Leading-Edge and Trailing-Edge flaps.

The main part of the X-31 aircraft model is a wing-fuselage section with eight servomotors for changing the canard angles ( $-70^\circ \leq \delta_c \leq 20^\circ$ ), the wing Leading-Edge inner/outer flaps ( $-70^\circ \leq \delta_{LEi} \leq 0^\circ$ ) / ( $-40^\circ \leq \delta_{LEo} \leq 0^\circ$ ), the wing Trailing-Edge flaps ( $-30^\circ \leq \delta_{TE} \leq 30^\circ$ ) and the rudder ( $-30^\circ \leq \delta_r \leq 30^\circ$ ) angles [3].

The X-31 aircraft is capable of flying at high angles of attack [ $-5^\circ$  to  $56^\circ$ ] and at sideslip angles [ $-20^\circ$  to  $20^\circ$ ].

The aircraft geometrical data are: reference wing area of 0.3984 m<sup>2</sup>, MAC of 0.51818 m, reference wing span of 1.0 m. In addition, its mass is 120 kg at Mach number of 0.18 and sea level. The variations of aerodynamic coefficients with angle of attack used in this analysis have been estimated using the Digital DATCOM code [4, 5].

### 3.1 Aircraft longitudinal motion analysis

If a longitudinal state vector  $\mathbf{x} = [u/V \ \alpha \ q \ \theta]^T = [x_1 \ x_2 \ x_3 \ x_4]^T$  is defined along with a single control term  $\delta$  (elevator), then the aircraft's linearized longitudinal dynamics becomes [6]

$$\dot{\mathbf{x}} = \mathbf{A}_{long} \mathbf{x} + \mathbf{B}_{long} \delta \quad (3)$$

where  $\mathbf{A}$  is the system matrix and  $\mathbf{B}$  is the control matrix.

The two pairs of complex conjugate roots of the linearized longitudinal dynamics correspond to short-period (fast mode) and phugoid (slow mode).

The non dimensional longitudinal equations of motion (1) are written, with  $x_1 = u/V$ ,  $x_2 = \alpha$ ,  $x_3 = q$  and  $x_4 = \theta$  as follows

$$\begin{cases} f_1 = a_1 (u/V) + a_2 \alpha + a_3 \theta + d_1 \delta \\ f_2 = a_4 (u/V) + a_5 \alpha + a_6 q + a_7 \theta + d_2 \delta \\ f_3 = a_8 (u/V) + a_9 \alpha + a_{10} q + d_3 \delta \\ f_4 = a_{11} q \end{cases} \quad (4)$$

where the coefficients  $a_1$  to  $a_{11}$  are determined with eqs (5)

$$\begin{cases} a_1 = X_u, a_2 = \frac{X_\alpha}{V}, a_3 = -\frac{g}{V} \cos \Theta_0, a_4 = \frac{V Z_u}{V - Z_{\dot{\alpha}}}, a_5 = \frac{Z_\alpha}{V - Z_{\dot{\alpha}}}, a_6 = \frac{V + Z_q}{V - Z_{\dot{\alpha}}}, \\ a_7 = -\frac{g}{V - Z_{\dot{\alpha}}} \sin \Theta_0, a_8 = \left( V M_u + \frac{V Z_u M_{\dot{\alpha}}}{V - Z_{\dot{\alpha}}} \right), a_9 = \left( M_\alpha + \frac{Z_\alpha M_{\dot{\alpha}}}{V - Z_{\dot{\alpha}}} \right), \\ a_{10} = \left( M_q + M_{\dot{\alpha}} \frac{V + Z_q}{V - Z_{\dot{\alpha}}} \right), a_{11} = 1, d_1 = \frac{X_\delta}{V}, d_2 = \frac{Z_\delta}{V - Z_{\dot{\alpha}}}, d_3 = \left( M_\delta + \frac{Z_\delta M_{\dot{\alpha}}}{V - Z_{\dot{\alpha}}} \right) \end{cases} \quad (5)$$

The term  $(u/V)$  is then replaced with  $\tilde{u}$ . By taking into account eqs (4) and (5) and knowing the term  $a_7 = 0$  (because  $\theta = 0$ ), the final total weight function  $W$  becomes:

$$\begin{aligned} W = \sum_{k=1}^4 w_k x_k f_k &= (w_1 a_1 \tilde{u}^2 + w_2 a_5 \alpha^2 + w_3 a_{10} q^2) + \alpha \tilde{u} (w_1 a_2 + w_2 a_4) + \\ &\alpha q (w_2 a_6 + w_3 a_9) + \tilde{u} (w_3 a_8 q + w_1 a_3 \theta) + w_4 a_{11} q \theta + \delta (w_1 d_1 \tilde{u} + w_2 d_2 \alpha + w_3 d_3 q) \end{aligned} \quad (6)$$

In order to analyse the sign of the total weight function  $W$ , it is needed to analyse the signs of all terms  $a_i, i = 1 \div 11$  and  $d_j, j = 1 \div 3$ .

For this reason, the graphs of the variations of coefficients  $a_1$  to  $a_{11}$  and  $d_1$  to  $d_3$  with angle of attack are shown in Figure 1, where it can be seen that the coefficients  $a_1 < 0, a_3 < 0, a_6 > 0, a_{11} > 0$  as well as other coefficients have fluctuant behaviour.

All three terms  $d_j$  have a oscillating behaviour.

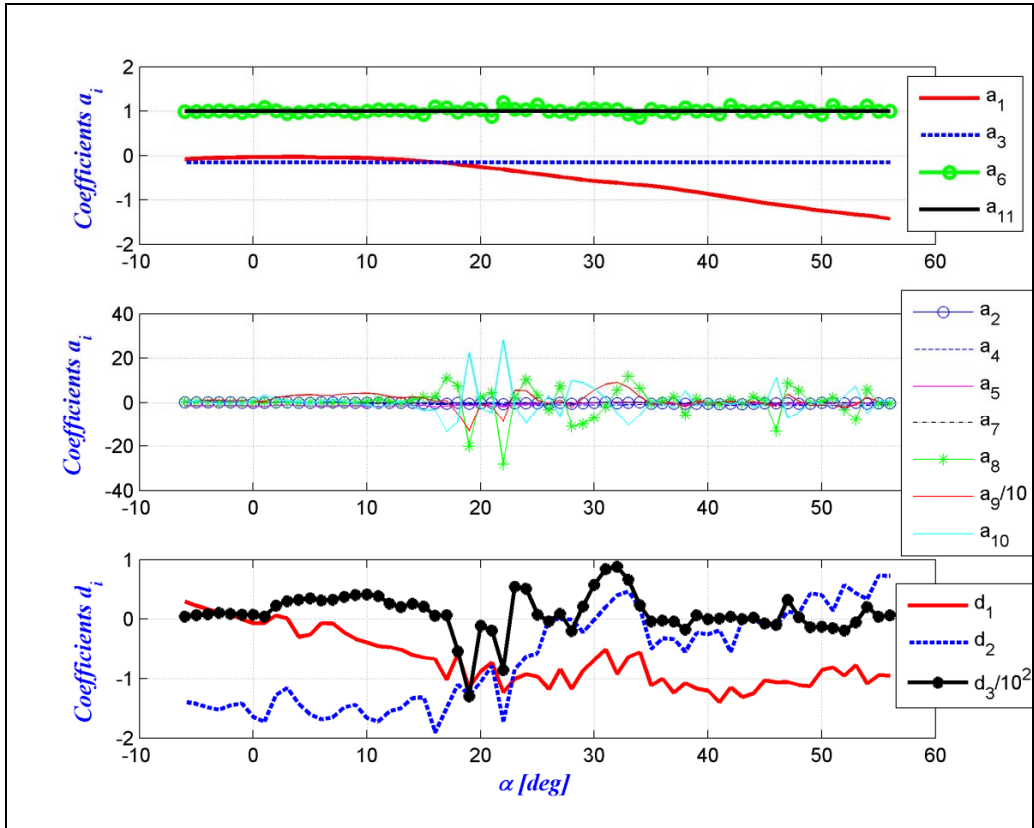


Figure 1 Coefficients  $a_i$  and  $d_j$  variation with the angle of attack

The weight functions are chosen considering the signs of the coefficients  $a_i, d_j$  and the tested cases for the pitch angles  $\theta = [-20 \text{ to } 20]^0$  and pitch rates  $q = [-10 \text{ to } 10]^0/\text{s}$ .

The aim of the  $WFM$  is to find 3 positive weighting functions  $w_1, w_2$  and  $w_3$  presented in Figure 2, based on the coefficients variations presented in Figure 1.

For the flight case configuration presented in this paper, it is considered that the canard angle  $\delta_c = 0^0$  and the flap angle  $\delta = 5^0$ .

The positive weight functions are defined as:

$$\begin{aligned}
 w_1 &= \tilde{u}(a_1 \tilde{u} + a_2 \alpha + a_3 \theta + d_1 \delta)^2 \\
 w_2 &= \alpha^2 (a_4 \tilde{u} + a_5 \alpha + a_6 q + d_2 \delta)^2 \\
 w_3 &= q^2 (a_8 \tilde{u} + a_9 \alpha + a_{10} q + d_3 \delta)^2 \\
 w_3 &= 1,100
 \end{aligned} \tag{7}$$

and the corresponding final form of the total weight function  $W$  is given by eq. (8).

$$W = \sum_{k=1}^4 w_k x_k f_k = w_1 f_1 \tilde{u} + w_2 f_2 \alpha + w_3 f_3 q + w_4 f_4 \theta = \tilde{u}^2 (a_1 \tilde{u} + a_2 \alpha + a_3 \theta + d_1 \delta)^3 + \alpha^3 (a_4 \tilde{u} + a_5 \alpha + a_6 \theta + d_2 \delta)^3 + q^3 (a_6 \tilde{u} + a_9 \alpha + a_{10} q + d_3 \delta)^3 + w_4 q \theta a_{11} \tag{8}$$

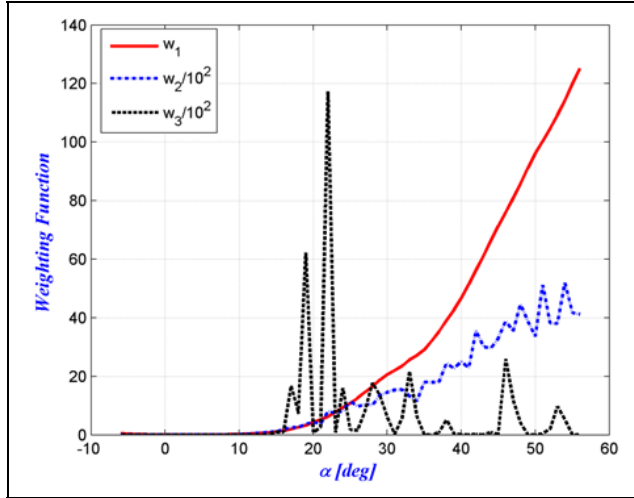
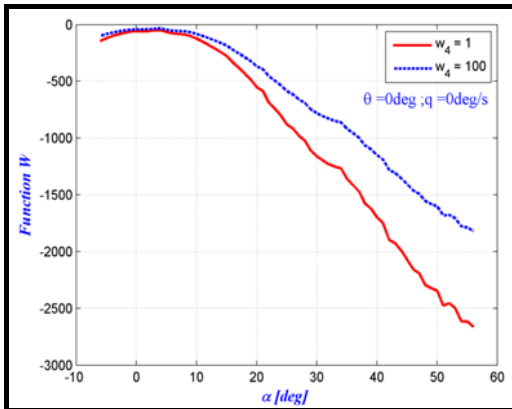
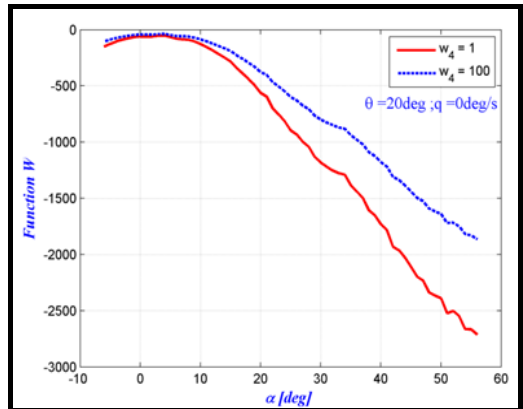


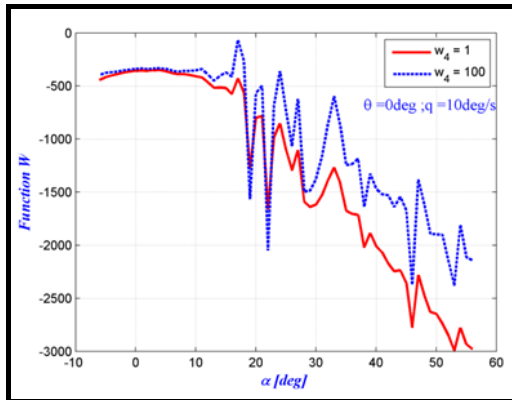
Figure 2 Weight functions chosen for longitudinal dynamics



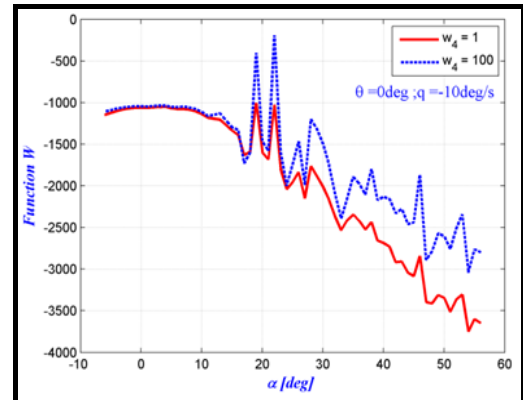
a)



b)



c)



d)

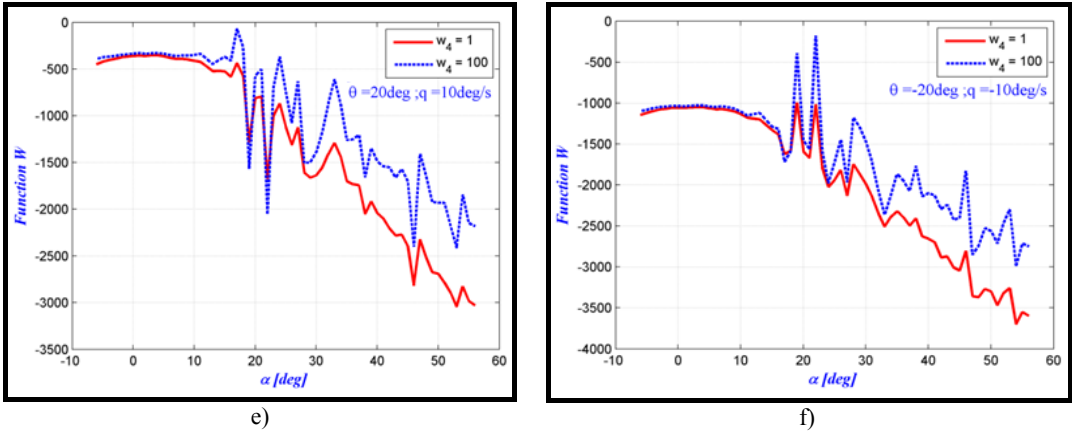


Figure 3 Stability analyses with the *weight functions method* for different values of constant  $w_4$  as a function of angle of attack

Two positives values for  $w_4$  are chosen: 1 and 100. It can be observed in Figure 3 that the shape of the stability curve does not change with the values of pitch angle  $\theta$  and pitch rate  $q$ , probably because the terms multiplying the pitch angle are small and constant ( $a_3 = 0.1601$  and  $a_{11} = 1$ ) as seen also on Figure 1; for this reason, their contributions are quite insignificant in comparison with the rest of the coefficients. Under these circumstances, for any considered range of pitch rates  $q$  and pitch angles  $\theta$  the system remains always stable.

### 3.2 Aircraft lateral analysis motion

Next, the non-dimensional lateral–directional equations of motion are given in eq. (9).

$$\begin{cases} \dot{\beta} = c_1\beta + c_2p + c_3\phi + c_4r + b_1\delta \\ \dot{p} = c_5\beta + c_6p + c_7r + b_2\delta \\ \dot{r} = c_8\beta + c_9p + c_{10}r + b_3\delta \\ \dot{\phi} = c_{11}p \end{cases} \quad (9)$$

where

$$\begin{cases} c_1 = \frac{Y_\beta}{V}, c_2 = \frac{Y_p}{V}, c_3 = \frac{g}{V} \cos \Theta_0, c_4 = \frac{Y_r - V}{V}, b_1 = \frac{Y_\delta}{V} \\ c_5 = G \left( L_\beta + N_\beta \frac{I_{xz}}{I_x} \right), c_6 = G \left( L_p + N_p \frac{I_{xz}}{I_x} \right), c_7 = G \left( L_r + N_r \frac{I_{xz}}{I_x} \right), \\ b_2 = G \left( L_\delta + N_\delta \frac{I_{xz}}{I_x} \right), c_8 = G \left( N_\beta + L_\beta \frac{I_{xz}}{I_z} \right), c_9 = G \left( N_p + L_p \frac{I_{xz}}{I_z} \right), \\ c_{10} = G \left( N_r + L_r \frac{I_{xz}}{I_z} \right), b_3 = G \left( N_\delta + L_\delta \frac{I_{xz}}{I_z} \right), c_{11} = 1 \end{cases} \quad (10)$$

The weighting function  $W$  can be thus written under the following form, where  $x_1 = \beta$  (sideslip rate),  $x_2 = p$  (roll rate),  $x_3 = r$  (yaw rate),  $x_4 = \phi$  (bank angle),  $x_5 = \delta$ :

$$W = \sum_{k=1}^4 w_k x_k f_k = w_1 \beta (c_1 \beta + c_2 p + c_4 r + c_3 \phi + \delta b_1) + w_2 p (c_6 p + c_5 \beta + c_7 r + \delta b_2) + w_3 r (c_{10} r + c_8 \beta + c_9 p + \delta b_3) + w_4 c_{11} p \phi \tag{11}$$

All possible positive and negative values of sideslip rate, roll rate, yaw rate and bank angle were considered. To analyse the sign of the weight function  $W$ , the sign of terms  $c_i, i = 1 \div 11$  and  $b_j, j = 1 \div 3$  where analyzed. In Figure 4, it can be observed that  $b_1, b_2, b_3 < 0, c_1, c_2, c_4, c_5, c_9 < 0$  and  $c_3, c_{11} > 0$ , while a non linear behaviour can be seen for the other four coefficients  $c_6, c_7, c_8$  and  $c_{10}$  presented.

In equation (11), the parenthesis which multiplies the first term is negative  $(c_1 \beta + c_2 p + c_4 r + c_3 \phi + \delta b_1)$ . For positive values of  $\beta$ , this term is always negative. We know that  $c_1 < 0$ , and for this reason the first weighting function  $w_1 = c_1^2 / \beta^2$ . Equation (11) becomes:

$$W = \frac{c_1^2}{\beta^2} \beta (c_1 \beta + c_2 p + c_4 r + c_3 \phi + \delta b_1) + w_2 p (c_6 p + c_5 \beta + c_7 r + \delta b_2) + w_3 r (c_{10} r + c_8 \beta + c_9 p + \delta b_3) + w_4 c_{11} p \phi \tag{12}$$

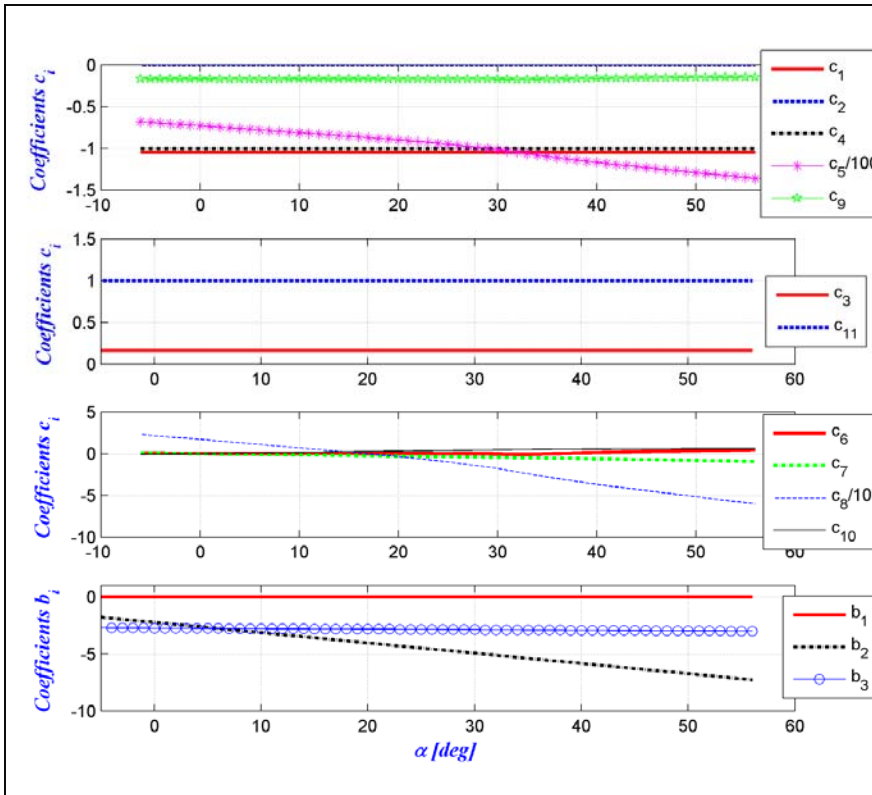


Figure 4 The  $c_i$  and  $b_j$  coefficients' variation with the angle of attack

The parenthesis which multiplies  $w_2 p$  is also negative  $(c_6 p + c_5 \beta + c_7 r + \delta b_2) < 0$ . Based on its sign the second function  $w_2$  are defined as  $w_2 = p^2 (c_6 p + c_5 \beta + c_7 r + \delta b_2)^2$ . The total function  $W$  is now given by eq. (13).

$$W = \frac{c_1^2}{\beta^2} \beta (c_1\beta + c_2p + c_4r + c_3\phi + \delta b_1) + p^2 (c_6p + c_5\beta + c_7r + \delta b_2)^2 \times \tag{13}$$

$$p(c_6p + c_5\beta + c_7r + \delta b_2) + w_3r(c_{10}r + c_8\beta + c_9p + \delta b_3) + w_4c_{11}p\phi$$

At this point it is possible to define  $w_3$  or  $w_4$  as a positive constant. Because  $c_{11} > 0$ , it was chosen  $w_4 = c_{11}p\phi$ . The final form of function  $W$  is given by eq. (14).

$$W = \frac{c_1^2}{\beta} (c_1\beta + c_2p + c_4r + c_3\phi + \delta b_1) + p^3 (c_6p + c_5\beta + c_7r + \delta b_2)^3 + \tag{14}$$

$$+ w_3r(c_{10}r + c_8\beta + c_9p + \delta b_3) + (c_{11}p\phi)^2 =$$

$$= c_1^3 + (c_2p + c_4r + c_3\phi + \delta b_1) \frac{c_1^2}{\beta} + c_{11}^2 p^2 \phi^2 + p^3 (c_6p + c_5\beta + c_7r + \delta b_2)^3 +$$

$$+ w_3r(c_{10}r + c_8\beta + c_9p + \delta b_3)$$

Two of the weighting functions chosen have a constant variation with angle of attack ( $w_1$  and  $w_4$ );  $w_2$  is variable and the last one is defined as  $w_3 = 1$  and 100.

It was considered that the roll rate  $p = [-6$  to  $6]^0/s$ , the yaw rate  $r = [-2$  to  $2]^0/s$ , the sideslip rate  $\beta = [-10$  to  $10]^0$  and the bank angle  $\phi = [-30$  to  $30]^0$ .

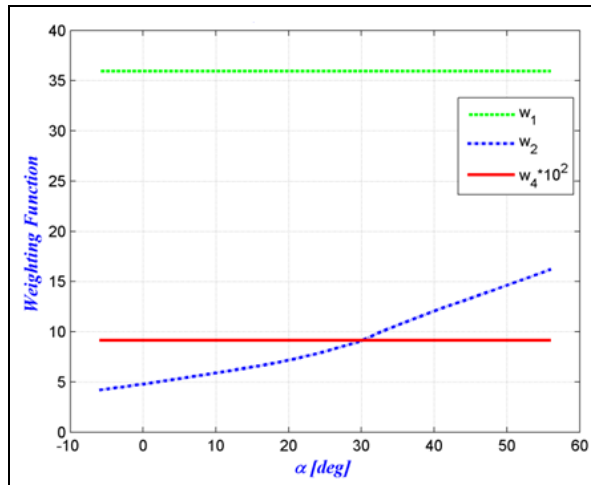
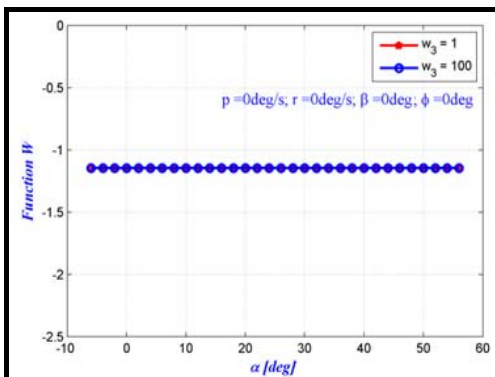
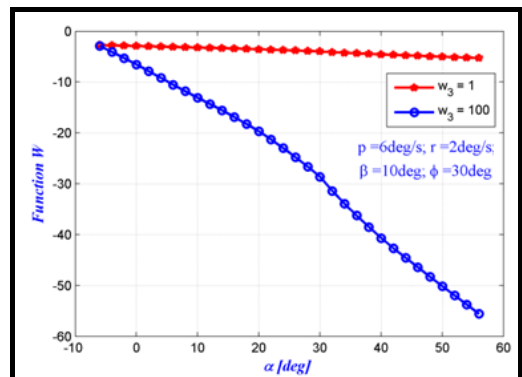


Figure 5 Weight functions chosen for the lateral dynamics



a)



b)



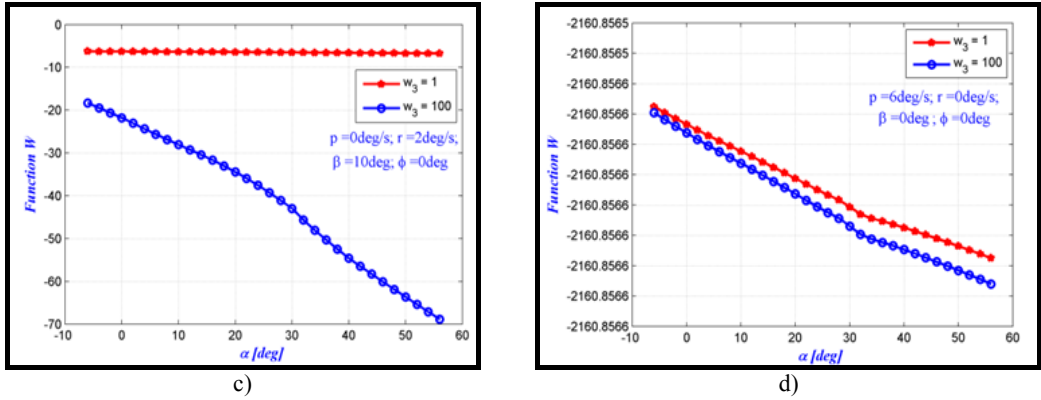


Figure 6 Lateral-Directional stability analysis with the *weight functions method* for different values of constant  $w_3$  as a function of angle of attack

For the lateral motion, the weight functions are overlapped only if  $p$ ,  $r$ ,  $\beta$  and  $\phi$  are zero; that means the value chosen for the weight function  $w_3$  have no influence on the total weight function  $W$ . The system is stable for roll, spiral and Dutch roll modes as the total weight function  $W$  is negative as shown in Figure 6 for extreme values chosen for  $p$ ,  $r$ ,  $\beta$  and  $\phi$ . For the studied case, the X-31 aircraft is stable for any type of motion within limits for  $p$ ,  $r$ ,  $\beta$ ,  $\phi$  (short-period, phugoid, roll, Dutch roll and spiral modes).

#### 4. ROOT LOCUS MAP

The five modes of motion for the X-31 aircraft are: the short period and the long period for longitudinal motion of the aircraft and the roll, Dutch roll and spiral for lateral motion. The natural frequency ( $\omega_n$ ) and the damping ratio ( $\zeta$ ) are defined for each mode from the values of the eigenvalues. For the longitudinal stability analysis, two modes are studied: the short period and the phugoid. The short term pitch is a second order response. The phugoid mode is the long-term motion of an aircraft after a disturbance.

The matrices of equation (3) are given in the next equation (15), as described in [6]:

$$\mathbf{A}_{long} = \begin{bmatrix} X_u & \frac{X_\alpha}{V} & 0 & -\frac{g}{V} \\ \frac{VZ_u}{V-Z_{\dot{\alpha}}} & \frac{Z_\alpha}{V-Z_{\dot{\alpha}}} & \frac{V+Z_q}{V-Z_{\dot{\alpha}}} & 0 \\ VM_u + \frac{VZ_uM_{\dot{\alpha}}}{V-Z_{\dot{\alpha}}} & M_\alpha + \frac{Z_\alpha M_{\dot{\alpha}}}{V-Z_{\dot{\alpha}}} & M_q + M_{\dot{\alpha}} \frac{V+Z_q}{V-Z_{\dot{\alpha}}} & 0 \\ 0 & 0 & 1 & 0 \end{bmatrix}, \quad (15)$$

$$\mathbf{x}_{long} = \begin{bmatrix} \Delta u \\ \Delta \alpha \\ \Delta q \\ \Delta \theta \end{bmatrix}, \quad \mathbf{B}_{long} = \begin{bmatrix} \frac{X_\delta}{V} \\ \frac{Z_\delta}{V-Z_{\dot{\alpha}}} \\ M_\delta + \frac{Z_\delta M_{\dot{\alpha}}}{V-Z_{\dot{\alpha}}} \\ 0 \end{bmatrix}, \quad \mathbf{u}_{long} = \Delta \delta_e$$

The roots of the characteristic equation  $\det(\lambda \mathbf{I} - \mathbf{A}_{long}) = 0$  gave these eigenvalues  $\lambda_1$  to  $\lambda_4$ .

For both longitudinal modes, the natural frequency  $\omega_n$  and damping ratio  $\zeta$  are estimated directly from the characteristic equation  $|\lambda \mathbf{I} - \mathbf{A}_{long}| = 0$ , as function of the longitudinal eigenvalues (eq. (16)); the eigenvalues  $\lambda_{1,2}$  correspond to short-period and  $\lambda_{3,4}$  to phugoid modes.

$$\begin{cases} \zeta \omega_n = |\operatorname{Re}(\lambda_{1,2})| \\ \omega_n \sqrt{1 - \zeta^2} = |\operatorname{Im}(\lambda_{1,2})| \end{cases}, \quad \begin{cases} \zeta \omega_n = |\operatorname{Re}(\lambda_{3,4})| \\ \omega_n \sqrt{1 - \zeta^2} = |\operatorname{Im}(\lambda_{3,4})| \end{cases} \quad (16)$$

A representation of the eigenvalues obtained for the longitudinal motion of an X-31 aircraft is shown in Figure 7. All real parts of eigenvalues are negative, which means that the X-31 aircraft is stable in its longitudinal motion.

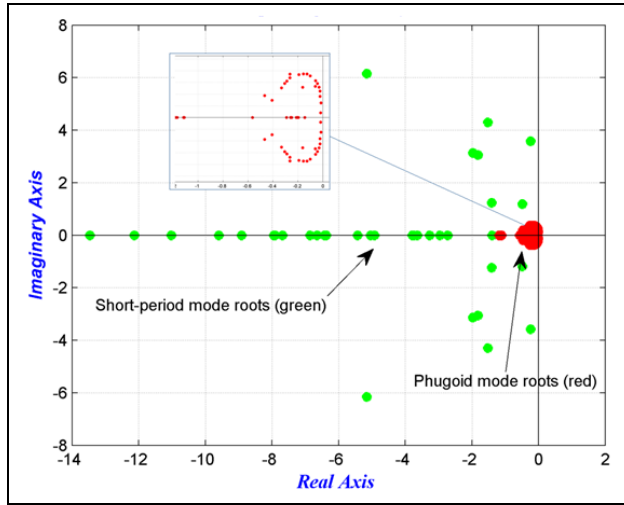


Figure 7 Root locus map longitudinal motion of the X-31 aircraft

The matrices of the aircraft lateral model are next defined in eq. (17), based on [6].

$$\mathbf{A}_{lat} = \begin{bmatrix} \frac{Y_\beta}{V} & \frac{Y_p}{V} & \frac{Y_r - V}{V} & \frac{g}{u_0} \cos \theta_0 \\ G \left( L_\beta + N_\beta \frac{I_{xz}}{I_x} \right) & G \left( L_p + N_p \frac{I_{xz}}{I_x} \right) & G \left( L_r + N_r \frac{I_{xz}}{I_x} \right) & 0 \\ G \left( N_\beta + L_\beta \frac{I_{xz}}{I_z} \right) & G \left( N_p + L_p \frac{I_{xz}}{I_z} \right) & G \left( N_r + L_r \frac{I_{xz}}{I_z} \right) & 0 \\ 0 & 1 & 0 & 0 \end{bmatrix}, \quad (17)$$

$$\mathbf{x}_{lat} = \begin{bmatrix} \Delta \beta \\ \Delta p \\ \Delta r \\ \Delta \varphi \end{bmatrix}, \quad \mathbf{B}_{lat} = \begin{bmatrix} \frac{Y_\delta}{V} \\ G \left( L_\delta + N_\delta \frac{I_{xz}}{I_x} \right) \\ G \left( N_\delta + L_\delta \frac{I_{xz}}{I_z} \right) \\ 0 \end{bmatrix}, \quad u_{lat} = \Delta \delta_a$$

Three modes are considered in the aircraft lateral motion modelling:

- Spiral mode representing, a convergent or a divergent motion;
- Roll mode representing a fast convergent motion, and
- Dutch roll mode representing a light damped oscillatory motion with a low frequency.

These modes are significant factors mainly in the uniform cruise flight. For the lateral aircraft motion modelling, two real roots correspond to roll and spiral modes, and a pair of complex roots correspond to Dutch roll mode obtained from the characteristic equation  $|\lambda \mathbf{I} - \mathbf{A}_{lat}| = 0$ . The rolling motion is generally very much damped and reaches the steady state in a very short time. An unstable spiral mode results into a turning flight path. The Dutch roll is a nuisance mode that appears in the basic roll response to lateral control and can induce non-controlled and non-desired motions in roll and yaw modes. These motions can significantly influence the ability of the pilot to control the lateral-directional motions with precision. The eigenvalues for all three motions described above for X-31 aircraft are represented in Figure 8: blue for Dutch Roll, red for spiral and green for roll mode.

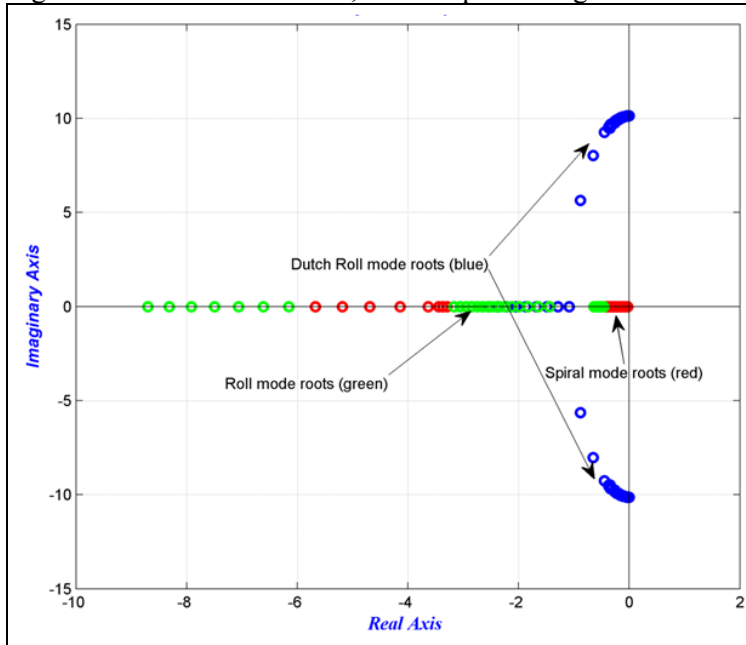


Figure 8 Root locus map for lateral motion

Results obtained with the *weight functions method* shown in Figure 6, have proven that the aircraft is stable in its lateral motion. Results presented with root locus map presented in Figure 8 show that the X-31 aircraft has a stable lateral motion, because all eigenvalues calculated with the root locus map are situated in the negative plane. The Handling Qualities Method could be used in further studies to determine the aircraft stability ([7], [8] and [9]).

## 5. CONCLUSIONS

A stability analysis based on the null solutions stability studies for differential equation systems was presented in this paper. The main aim was to found the positive weight functions in order to analyze the X-31 aircraft stability. The aerodynamics coefficients and their stability derivatives were determined with Digital DATCOM code. Based on the aircraft's aerodynamic model in the WFM, 3 functions were defined as function of stability

derivatives terms, and the last fourth function was considered positive and chosen to be 1 and 100. The WFM was applied for longitudinal and lateral motions. A discussion of results was done for each case, and the stability was defined and is summarized in the previous sections. HQM was also applied to validate the aircraft stability results found with WFM.

X-31 has a stable longitudinal and lateral dynamics. For the considered altitude and Mach number, the aircraft was found to be stable, regardless the angle of attack. Both modes tested here, the slow and the fast, did not induced any oscillations and/or instabilities.

### ACKNOWLEDGMENTS

Thanks are due to Dr. Andreas Schütte from DLR and Dr. Russell Cummings from the USAF Academy for their leadership and support in RTO/AVT-161 “Assessment of Stability and Control Prediction Methods for NATO Air and Sea Vehicles” and for providing the wind tunnel test data for the X-31 aircraft.

### REFERENCES

- [1] The USAF Stability And Control Digital Datcom, Volume I, *Users Manual. USAF Technical Report AFFDL-TR-79-3032 (AD A086557)*, April 1979.
- [2] I. Stroe, *Weight functions method in stability study of vibrations*, SISOM 2008 and Session of the Commission of Acoustics, Bucharest 29–30 May, 2008.
- [3] I. Stroe and P. Parvu, *Weight functions method in Stability Study of Systems*, 79<sup>th</sup> Annual Meeting of the International Association of Applied Mathematics and Mechanics (GAMM), Bremen, pp. 10385–10386, 2008.
- [4] N. Anton, R. M. Botez and D. Popescu, *Stability derivatives for X-31 delta-wing aircraft validated using wind tunnel test data*, Proceeding of the Institution of Mechanical Engineers, Vol. **225**, Part G, Journal of Aerospace Engineering, pp 403-416, 2011.
- [5] N. Anton, R. M. Botez and D. Popescu, New methodology and code for Hawker 800XP aircraft stability derivatives calculations from geometrical data, *The Aeronautical Journal*, Vol. **114**, No. 1156, Paper No. 3454, 2010.
- [6] L. V. Schmidt, Introduction to Aircraft Flight Dynamics, *AIAA Education Series*, 1998.
- [7] J. Hodgkinson, Aircraft Handling Qualities, *AIAA Education Series*, 1999.
- [8] W. Bihrlé, *A Handling Qualities Theory for Precise Flight Path Control*, Tech. Rep. *AFFDL-TR-65-195*, AFRL, Wright Patterson AFB, OH, June 1965.
- [9] Christoffer M. Cotting, *Evaluation of flying qualities analysis: Problems for the new generation of aircraft*, PhD Thesis, Faculty of the Virginia Polytechnic Institute and State University, Blacksburg, Virginia, March 2010.

### NOMENCLATURE

$b$	wing span
$\bar{c}$	wing mean aerodynamic chord
$C_D$	drag coefficient
$C_{D\alpha}$	drag due to the angle of attack derivative
$C_{Dq}$	drag due to the pitch rate derivative
$C_L$	lift coefficient
$C_{L\alpha}$	lift due to the angle of attack derivative
$C_{Lq}$	lift due to the pitch rate derivative
$C_{L\dot{\alpha}}$	lift due to the angle of attack rate derivative
$C_m$	pitching moment coefficient
$C_{m\alpha}$	static longitudinal stability moment with respect to the angle of attack derivative
$C_{mq}$	pitching moment due to the pitch rate derivative

$C_{m\dot{\alpha}}$	pitching moment due to the angle of attack rate derivative
$C_{lp}$	rolling moment due to the roll rate derivative
$C_{lr}$	rolling moment due to the yaw rate derivative
$C_{l\beta}$	rolling moment due to the sideslip angle derivative
$C_{l\dot{\beta}}$	rolling moment due to the sideslip angle rate derivative
$C_{np}$	yawing moment due to the roll rate derivative
$C_{nr}$	yawing moment due to the yaw rate derivative
$C_{n\beta}$	yawing moment due to the sideslip angle derivative
$C_{yp}$	side force due to the roll rate derivative
$C_{yr}$	side force due to the yaw rate derivative
$C_{y\beta}$	side force due to the sideslip angle derivative
$I_x, I_y, I_z$	moment of inertia about the X, Y and Z body axes, respectively
$I_{xz}$	product of inertia
$L_p$	rolling moment due to roll rate $L_p = \frac{\tilde{q}Sb}{I_x} \left( \frac{b}{2V} \right) C_{lp}$
$L_r$	rolling moment due to yaw rate $L_r = \frac{\tilde{q}Sb}{I_x} \left( \frac{b}{2V} \right) C_{lr}$
$L_\beta$	rolling moment due to sideslip $L_\beta = \frac{\tilde{q}Sb}{I_x} C_{l\beta}$
$L_\delta$	roll control derivative $L_\delta = \frac{\tilde{q}Sb}{I_x} C_{l\delta}$
$m$	aircraft mass
$M$	Mach number
$M_q$	pitching moment due to pitch rate $M_q = \frac{\tilde{q}S\bar{c}}{I_y} \frac{\bar{c}}{2V} C_{m_q}$
$M_u$	pitching moment increment with increased speed $M_u = \frac{\tilde{q}S\bar{c}}{I_y} C_{m_M}$
$M_\alpha$	pitching moment due to incidence $M_\alpha = \frac{\tilde{q}S\bar{c}}{I_y} \frac{\bar{c}}{2V} C_{m_\alpha}$
$M_{\dot{\alpha}}$	pitching moment due to rate of change of the incidence $M_{\dot{\alpha}} = \frac{\tilde{q}S\bar{c}}{I_y} \frac{\bar{c}}{2V} C_{m_{\dot{\alpha}}}$
$M_\delta$	pitching moment due to flap deflection $M_\delta = \frac{\tilde{q}S\bar{c}}{I_y} C_{m_\delta}$
$N_p$	yawing moment due to roll rate $N_p = \frac{\tilde{q}Sb}{I_z} \left( \frac{b}{2V} \right) C_{n_p}$
$N_r$	yawing moment due to yaw rate $N_r = \frac{\tilde{q}Sb}{I_z} \left( \frac{b}{2V} \right) C_{n_r}$
$N_\beta$	yawing moment due to sideslip $N_\beta = \frac{\tilde{q}Sb}{I_z} C_{n_\beta}$

$N_\delta$	yawing moment due to flap deflection $N_\delta = \frac{\tilde{q} S b}{I_z} C_{n_\delta}$
$p, q, r$	angular rates about the X, Y and Z body axes, respectively
$\dot{p}, \dot{q}, \dot{r}$	time rate of change of $p, q, r$
$q_\infty$	dynamic pressure
$S$	wing area
$u$	axial velocity perturbation
$\dot{u}$	time rate of change of $u$
$V$	airspeed
$X_u$	drag increment with increased speed $X_u = -\frac{\tilde{q} S}{mV} 2C_D$
$X_\alpha$	drag due to incidence $X_\alpha = \frac{\tilde{q} S}{m} (C_L - C_{D_\alpha})$
$X_\delta$	drag due to flap deflection $X_\delta = -\frac{\tilde{q} S}{m} C_{D_\delta}$
$Y_p$	side force due to roll rate $Y_p = \frac{\tilde{q} S}{m} \left( \frac{b}{2V} \right) C_{y_p}$
$Y_r$	side force due to yaw rate $Y_r = \frac{\tilde{q} S}{m} \left( \frac{b}{2V} \right) C_{y_r}$
$Y_\beta$	side force due to sideslip $Y_\beta = \frac{\tilde{q} S}{m} C_{y_\beta}$
$Y_\delta$	side force control derivative $Y_\delta = \frac{\tilde{q} S}{m} C_{y_\delta}$
$Z_q$	lift due to pitch rate $Z_q = -\frac{\tilde{q} S}{m} \frac{\bar{c}}{2V} C_{L_q}$
$Z_u$	lift due to speed increment $Z_u = -\frac{\tilde{q} S}{m} 2C_L$
$Z_\alpha$	lift due to incidence $Z_\alpha = -\frac{\tilde{q} S}{m} (C_D + C_{L_\alpha})$
$Z_{\dot{\alpha}}$	lift due to the rate of change of incidence $Z_{\dot{\alpha}} = -\frac{\tilde{q} S}{m} \frac{\bar{c}}{2V} C_{L_{\dot{\alpha}}}$
$Z_\delta$	lift due to flap deflection $Z_\delta = -\frac{\tilde{q} S}{m} C_{L_\delta}$
$\alpha$	angle of attack
$\dot{\alpha}, \dot{\beta}, \dot{\theta}$	time rate of change of $\alpha, \beta, \theta$
$\beta$	sideslip angle
$\delta$	control deflection
$\theta$	pitch angle
$\phi$	roll angle